Quadrilateral mesh of non-simply connected domain and non-planar surfaces from a given cross-field

Kokou Dotse, Vincent Mouysset, Sébastien Pernet

Abstract In this paper, we present a method for constructing a quad mesh from an initial cross-field given by the user. The idea of this approach is to provide a framework to process any cross-field in order to generate a quad mesh and thus benefit from the properties of the field in the resulting mesh. With this point of view, we handle the case of non-simply connected domains and we also address the notion of singular point placement on the edge, which allows us to handle geometries of arbitrary index. Finally, we give an extension of the method to non-planar surface manifolds.

1 Introduction and Related work

Several numerical schemes used for numerical simulation are based on the implementation of a quadrilateral or hexahedral mesh, as they offer numerous advantages. In mechanics, quadrilaterals are interesting because similar results can be obtained by using modified first-order quadrilaterals instead of quadratic simplexes. Similarly, for the propagation of electromagnetic waves, we observe that quadrilaterals are very efficient due to their naturally tensorial structure [1]. In fluid mechanics, quadrilaterals provide a simple way to deal with anisotropic phenomena within boundary layers [1]. However, while the generation of symplectic meshes (triangles, tetrahedrons) has been well developed for more than half a decade, while the generation of quadrilaterals or hexahedrons is more problematic. Actually it is difficult to simultaneously respect every constraint required by the properties of a good hexahedral mesh, align-

Kokou Dotse
ONERA, 2 Av. Edouard Belin, 31000 Toulouse, France, e-mail: kokou.dotse@onera.fr

Vincent Mouysset
ONERA, 2 Av. Edouard Belin, 31000 Toulouse, France, e-mail: vincent.mouysset@onera.fr

Sébastien Pernet
ONERA, 2 Av. Edouard Belin, 31000 Toulouse, France, e-mail: sebastien.pernet@onera.fr

ment of elements with the edge of the domain, size of elements, and mesh quality (see [2]).

Among methods developed to create quadrilateral meshes, such as tri-to-quad conversion [3], SQuad [4], Blossom-Quad [5], the Cartesian grid method [6], the method of frontal advance (also called the paving method) [7, 8], and medial-axis based decomposition methods [9, 10], an interesting one is based on cross-fields analysis [2]. The idea involving cross-fields is to simulate orientation properties of quadrilaterals to derive a proper partitioning of the domain into four-sided subdomains. They are used for the first time in computer graphics applications to control surface mapping for non-photorealistic rendering, texture synthesis and remapping, and global parameterization [11, 12, 13]. A cross-field is a field structure that binds each point of the domain to "a cross", i.e. a given vector and its rotations with an angle of $k\frac{\pi}{2}$, where $k \in [\![0, 3]\!]$. In [2], the authors generate such cross-fields by propagating the crosses from the outer normal of the domain from the edge of the domain (see details in [2]). In [14], the authors addresses constructing quad-mesh on surface patches and in [15], the quad-mesh generation on manifold surfaces is discussed. One goal is to build a smooth cross-field that is aligned with the domain boundary. In the literature, the approach often used consists in minimizing an energy that characterizes the variations of the cross-field [16].

$$\inf_u E(u) = \frac{1}{2}\int_\Omega |\nabla u|^2 dA + \frac{1}{4\epsilon^2}\int_\Omega (|u|^2 - 1) dA. \tag{1}$$

The solution field of (1) is used to guide the generation of the quadrilateral mesh. To do this, field lines are integrated from the singular points of the cross-field. These field lines called separators allow to partition the domain into regions of 4 sides that are then filled with quadrilateral meshes (see Figure 1).

The mesh obtained then depends on the location of the singular points (corners of subdomains) in the cross-field. Unfortunately, this distribution can sometimes lead to invalid or unintended partitioning. The first one notably occurs on ultra-stretch domains. The second one refers to partition shapes leading to resulting cell sizes that are widely inhomogeneous (see Figure 2). In other words, we do not control the appearance of singular points nor their distribution.To bypass these problems, one should aim at controlling the kind and location of singular points in the cross-field.

To do this, one can see that a generator of quadrilateral mesh can be achieved by analyzing how cross-fields are related to the Ginzburg-Landau energy, as studied in [16, 17]. Jezdimirović and al [18] propose an algorithm based on a user-defined singularity model as input, possibly with high valence singularities. Alexis Macq and al [19] give a formulation of the Ginzburg-Landau energy allowing the imposition of internal singularities by substituting them with little holes drilled in the domain. The Ginzburg-Landau energy of the crossed field on the drilled domain is then calculated by solving a linear Neumann problem. They also propose a reformulation of the Ginzburg-Landau energy to handle boundary singularities. However, the complex framework of the Ginzburg-landau theory does not allow to easily take into account

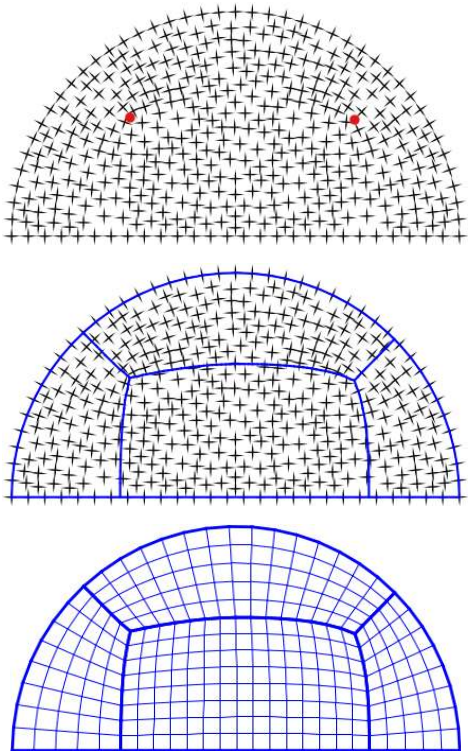

Fig. 1 Quad mesh from Ginzburg-Landau Energy

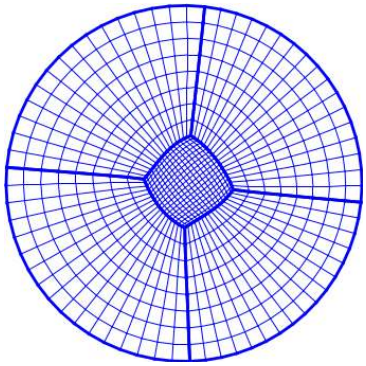

Fig. 2 Inhomogeneous mesh

non-planar geometry. Moreover additional problems arising from usual industrial meshing context such as handling with piecewise materials, piecewise inhomogeneous boundary conditions or non-analytic geometry, are not suitably addressed by these methods.

The idea we propose to develop in this paper is to consider the cross-field as an independent input for the meshing method, thus allowing us to look for a better candidate. On one hand, we can expect different singular point distributions (and thus more homogeneous meshes), an easier partitioning on non-planar surfaces, and a tool to address non-simply connected domains. On the other hand, some properties will have to be formulated to ensure that the cross-field leads to a full quad mesh, and operations must be performed on the cross-field to satisfy some boundary conditions arising from partitioning and handling of non-simply connected domains.
To illustrate the purpose of this article, we consider an eigenmode of the Laplacian as an example in Figure 3. The cross-field is constructed from the quarter angle of the gradient of this eigenmode (the same construction can be applied to isolines). We observe that the extrema of an eigenmode of the Laplacian, and therefore of the corresponding cross-field, on the domain are equidistant from the boundary and from one another. This results in a more homogeneous mesh using our method.

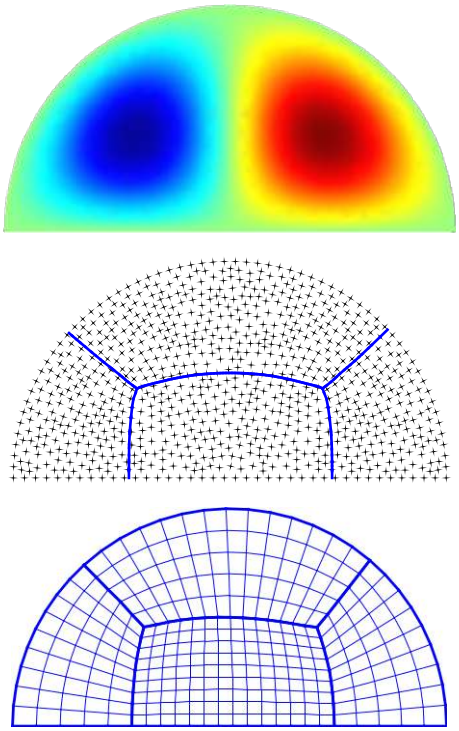

Fig. 3 A quadrilateral mesh constructed from eigenmode solutions.

Another example is given by Viertel et al. in [16], and in most Ginzburg-Landau based quad mesh papers, as the first step of the process. Cross-fields are obtained from representation fields given in the complex plane by:

$$z \in \mathbb{C} \longmapsto \prod_i \left(\frac{(z - a_i)}{|z - a_i|} \right)^{\frac{d_i}{4}} \in \mathbb{C}, \tag{2}$$

where each $a_i \in \mathbb{C}$ is a singular point of the field and $d_i/4$ its associated index. The same construction as previously is performed and the resulting cross-field and final mesh are depicted in Figure 4. It can be noted that the fields in equation (2) are not straightforwardly used in [16], but a correction process is first applied to enforce a prescribed alignment. Our method will thus propose an alignment phase that works similarly to this step.

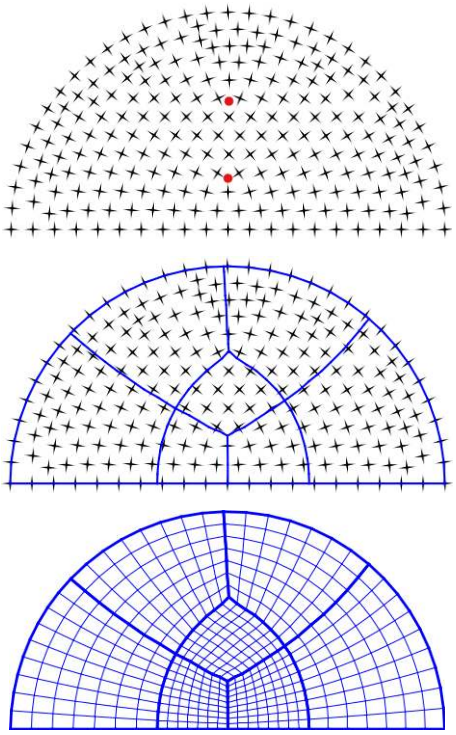

Fig. 4 A quadrilateral mesh constructed from the cross-field of equation (2). Singular points a_i are plotted in red.

The remainder of this paper is organized as follows. First, in section 2, we introduce some mathematical notions used to express the constraints required on a field of crosses for the generation of quadrilateral meshes, discuss the alignment of a given field of crosses with respect to the domain boundaries for planar domains, and address the notion of singular border points. We then extend the method to non-simply connected domains in section 3. Finally, in section 4, we discuss the case of non-planar surfaces, whose main difficulty is the absence of a global reference frame.

2 Quadrilateral mesh from a cross-field

For any given domain Ω, the idea is to find a subdivision of Ω into subdomains with four sides. Suppose that we can partition Ω using the field lines of a vector field defined on Ω. To establish regions, it is imperative to guarantee that the streamlines (definition in section 2.1), can intersect each other. To this aim, we use a particular vector field called a cross-field. A cross-field is a map that associates four directions orthogonal to each other to each point (see section 2.1). By constructing the cutting of Ω with streamlines whose origins are the singular points of the cross-field, we can create partitions that do not contain any singular points. Let D be a partition obtained in such a way. The only singular points of the field included in D then coincide with the corners of D. Applying the Poincare-Hopf theorem (see [16]), it follows that D has necessarily four corners, i.e. it is a four-sided domain. Meshing with quads a four-sided domain is trivial. For instance, we can use transfinite interpolation (see [20]) to generate a regular mesh on a domain with four sides. Finally, we achieve a quad mesh of whole domain (see Figure 1).

Lately, as announced in the introduction, in this paper we would like to have the possibility to choose any cross-field and use it to generate a quadrilateral mesh. Contrary to the classical approach of directly generating a cross-field aligned with the edge of the domain, we would rather act on any cross-field provided on the domain. The advantage of such a choice would be that the generated mesh can be aligned with the chosen field, thus making the mesh inherit the properties of the cross-field.

Throughout this section, we will assume that Ω is a bounded, connected domain in $\mathbb{R}^2$ with a piecewise-smooth boundary.

2.1 Cross-fields definition

A two dimensional cross is defined by:

$$c(\theta) = \{(cos(\theta + k\pi/2), \sin(\theta + k\pi/2)), k \in [[0; 3]]\} \tag{3}$$

Let $C = \{c(\theta), \theta \in \mathbb{R}\}$. By associating to each point p of Ω an angle $\theta(p)$, we define the cross-field on Ω as a map $u : p \in \Omega \longmapsto c(\theta(p)) \in C \cup \{0\}$ and which eventually vanishes at a finite number of points, called the singular points.

Let c_0 be the cross formed by the x-axis and the y-axis of a local planar coordinate system, for a cross $u(p)$ given at a point $p \in \Omega$, its principal angle $\theta_u(p)$ is given by the minimal rotation between c_0 and u, i.e.:

$$\theta_u(P) = \min_{\theta}\{\theta \in \mathbb{R}/u = R(\theta)c_0\}, \tag{4}$$

where $R(\theta)$ denotes the rotation of angle θ.

Given $\gamma(s)$, with $s \in [0,1]$, be a C^1 curve parametrized on the domain Ω, and let $\partial\gamma(s)$ denote its derivative. We say that γ is a streamline of u if, for all $s \in [0,1]$, there exists $k \in [\![1,4]\!]$ such that the cross-product $\partial\gamma(s) \wedge u^k(\gamma(s)) = 0$. Here, $u^k(\gamma(s)), k \in [\![1,4]\!]$ refers to the branches of the cross-field u at point $\gamma(s)$. A separatrix of a cross-field is a streamline that begins or ends at a singularity.

2.2 Index

A number called the index, noted id_u, is associated with each singular points. It quantifies the number of times the field turns onto itself around the point p. At any point $p \in \Omega \backslash \partial\Omega$, it is evaluates as (see [17]):

$$id_u(p) = \frac{1}{2\pi} \int_\gamma d\theta_u, \tag{5}$$

where $\gamma : [0,1] \longrightarrow \Omega$ is a simple closed curve around p containing no other singular point. Note that if p is not singular, $id_u(p) = 0$.

Applying equation (5) with respect to $\partial\Omega$, we can define the following global quantity on u (see section 2.3):

$$deg(u, \partial\Omega) = \frac{1}{2\pi} \int_{\partial\Omega} d\theta_u, \tag{6}$$

which will allow the following to define a general constraint on the initial cross-field. In the literature, $deg(u, \partial\Omega)$ is commonly referred to as the Brouwer degree.
These points are later chosen to be the origin of the streamlines used to partition the domain. Practically, as done for instance in [2], we build the separatices from every singular point and apply a merging algorithm to avoid doubling of lines due to numerical errors.

As exposed previously, singular points will be used as starting points for separatrices. Hence, to define how many separatrices start with each point p, we introduce the valence of p, denoted $V(p)$. It is directly related to the index of the point in the cross-field and is given by:

$$V(p) = 4 - 4id_u(p). \tag{7}$$

2.3 Compatibility constrain on the cross-field

The Poincaré-Hopf theorem allows us to relate the vector field to the topology of the domain. This theorem can be extended in the context of cross-field (see [21]). It states that, for a cross-field u defined on a domain and whose boundary crosses are aligned with the outgoing normal of the domain, we have the following relation:

$$\sum_{i=1}^{n} id_u(p_i) = \chi(\Omega), \tag{8}$$

where $(p_i)_{i\in\{1,\dots,n\}}$ is the set of singular point of u and $\chi(\Omega) = 2 - 2g - b$, ($g$ is genus of Ω, b is boundary number of Ω) is characteristic Euler of Ω.

Taking into account the boundary and interior singular points, the formula (8) becomes:

$$\sum_{i=1}^{n_s} id_u(s_i) + \sum_{i=1}^{n_b} id_u(b_i) = \chi(\Omega), \tag{9}$$

where $(s_i)_{i\in\{1,\dots,n_s\}}$ is the set of interior singular point of u and $(b_i)_{i\in\{1,\dots,n_b\}}$ is a boundary singular point of u.

As derived from formula 6, it follows that:

$$\deg(u, \partial\Omega) = \sum_{i=1}^{n_s} id_u(s_i). \tag{10}$$

Finally, we deduce a compatibility constraint that our cross-field must respect on Ω with the following formula:

$$deg(u, \partial\Omega) = \chi(\Omega) - \sum_{i=1}^{n_b} id_u(b_i). \tag{11}$$

2.4 Alignment of cross-field

From the example pictured on Figure 3, we see that the proposed cross-field has the correct properties. Indeed, on the one hand, the sum of the indexes of the field is equal to 1 and the domain has two singular boundary points of index 1/4 each. Relation (11) is verified.
However, when using a cross-field method (summarized at the beginning of section 2) to partition the domain, it is noted that some subdomains deviate from the typical quadrilateral shape, as shown in Figure 5. This deviation is a result of the cross-field not being properly aligned with the boundaries of the domain, which is in violation of the assumptions of the Poincaré-Hopf theorem. As a result, some partitions do not have four sides.

To address this issue, we will adjust the cross-field to align it with the boundaries of the domain. Given a cross-field according to the formula (11), the task is to find a way to align this cross-field with the boundaries of the domain without altering its initial properties. This can be achieved by finding a scalar field ϕ representing rotation angles and initial cross-field. Thus we denote the new cross-field:

$$v = R(\phi)u, \tag{12}$$

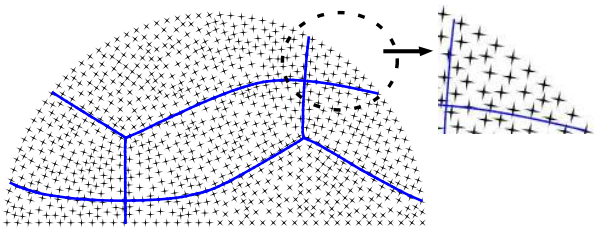

Fig. 5 Invalid partitioning obtained from rough cross field extraction of modal solution plotted on first picture on figure 3

and we want to obtain $v = N$ on $\partial\Omega$, where $R(\phi)$ is given by the equation:

$$R(\phi) = \begin{pmatrix} cos(\phi) & -sin(\phi) \\ sin(\phi) & cos(\phi) \end{pmatrix}, \tag{13}$$

and N is the cross-field associated with the outgoing normal. Our determination of ϕ is based on the approach of [16]. It entails continuously propagating the angle difference between u and N throughout Ω via the following equation:

$$\begin{cases} \triangle\phi \quad\quad = 0 \text{ in } \Omega, \\ \phi(\gamma(t)) = \tilde{\phi}(\gamma(t)) + \sum_{i=1}^{n_b} \delta\theta(b_i)\mathbb{1}_{\gamma([0,t])}(b_i), \quad \forall t \in [0,1]. \end{cases} \tag{14}$$

In this equation,

- $\gamma : [0,1] \longrightarrow \partial\Omega$ is a parameterization of $\partial\Omega$ such that $\gamma(0)$ is not a boundary singular point and $\gamma(0) = \gamma(1)$,
- $\tilde{\phi} = \theta_N - \theta_u$. This quantity is calculated continuously along $\partial\Omega$,
- $\delta\theta(b_i)$ quantifies the presence of singular points b_i. This concept is covered in depth in section 2.5,
- $\mathbb{1}_{\gamma([0,t])}$ denotes the indicator function.

It can be proven that $\phi(\gamma(0)) = \phi(\gamma(1))$ and that $\forall p \in \bar{\Omega}$, $id_v(p) = id_u(p)$.

Applying this method to the cross-field of Figure 5, we achieve the partitioning illustrated in Figure 6. An additional illustration of this procedure on a different domain can be seen in Figure 7.

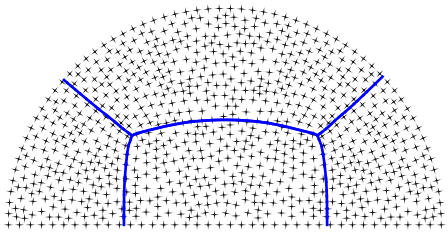

Fig. 6 Cross-field of the figure 5 after alignment process (same picture as second one on figure 3)

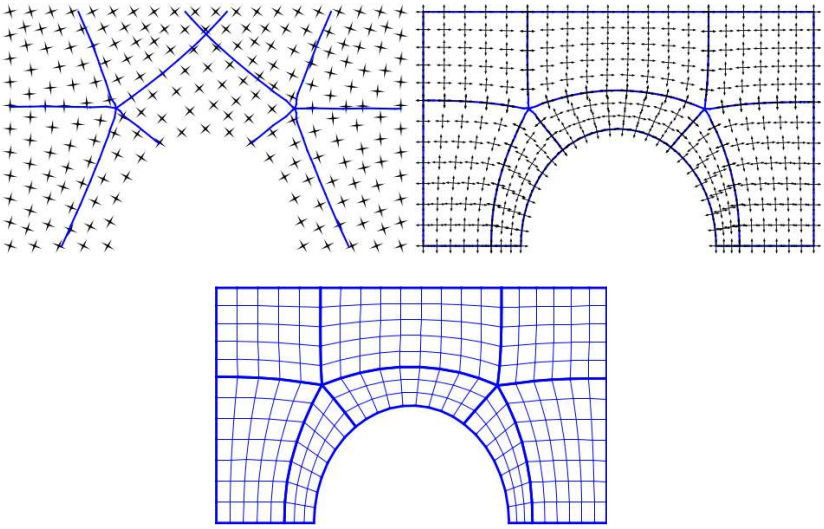

Fig. 7 Top: unaligned cross-field, middle: rectified cross-field, bottom: mesh quad

2.5 Boundary singularities

It is sometimes mandatory for numerical simulations, to delimit portions of the domain boundary with physical nodes. This is especially the case when applying piecewise boundary conditions. When these nodes do not coincide with the geometrical ones (as corners), one way to include this information would be to see them in the cross-field as singular points of the boundary.

The presence of a boundary singularity should indicate a local rotation of the cross associated with the outgoing normal. The quantification of this rotation would thus give the value of the index associated with the singularity. In the literature, the associations (corner angle - index) proposed tend to minimize the rotation of the field on the boundary in order to keep the cross-field inside the domain as smooth as possible. The conventional distribution proposed in the literature corresponds to the values in table 1 with different tolerances around the given angles (see details in [19]).

angle	$\pi/4$	π	$3\pi/2$
index	$1/4$	0	$-1/4$

Table 1 Usual distribution of angles of boundary singularities [19].

By applying (5) to a boundary singular point b, we get the following formula:

$$\delta\theta_u(b) = 2\pi I(b) - \pi + \widehat{b}, \tag{15}$$

where $\delta\theta_u(b)$ denotes the effective prescribed angular rotation of the cross-field at the neighborhood of b corresponding to a given index $I(b)$ and $\widehat{b}$ is the measure of the boundary open angle at corner b.

We illustrate on figures 8 and 9 impact on resulting meshes for several choices of arbitrary boundary singularity.

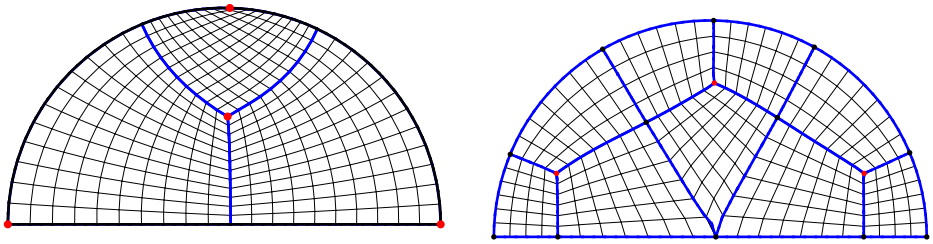

Fig. 8 Top: 3 border singular points of index 1/4 each and 1 internal singular point of index 1/4; Bottom: 2 singular points of index 1/4 and 1 singular point of index -1/4 and 3 singular points of index 1/4 inside the domain

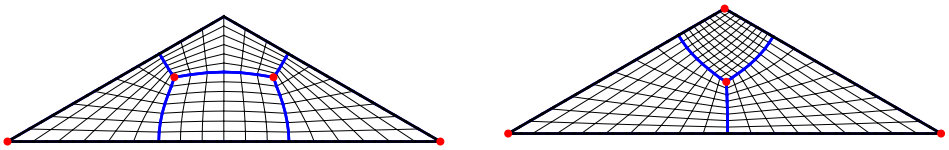

Fig. 9 Top: 2 border singular points of index 1/4 each and 2 internal singular point of index 1/4; Bottom: 3 singular points of index 1/4 and 1 singular point of index 1/4 inside the domain

3 Non-simply connected domains

In this section, we will further explore the application of the previously developed alignment method to more complex domains, specifically those containing holes. The application of this method to complex domains with holes is a crucial step towards achieving accurate and reliable results in multi-material domain treatment.

Let Ω be a non-simply connected domain such that $\partial\Omega = \bigcup_{i=1}^{n_\Gamma} \Gamma_i$, where Γ_i represents a simply connected component of the boundary $\partial\Omega$ and n_Γ is the number of such simply connected components. By applying formula (11), it is observed that the constraint on the initial cross-field becomes:

$$deg(u, \partial\Omega) = \sum_{i=1}^{n_\Gamma} deg(u, \Gamma_i) = \chi(\Omega) - \sum_{c \in \partial\Omega} id_u(c), \tag{16}$$

However, when dealing with non-simply connected domains, this condition is only a requirement and not a guarantee, as it does not ensure continuity of ϕ (the alignment angle developed in the previous section) on each boundary segment separated by the singular points on each $\Gamma_i,\ i \in \{1, n_\Gamma\}$. To address this issue, we impose condition (11) on each $\Gamma_i,\ i \in \{1, n_\Gamma\}$, leading to the following formula:

$$\begin{cases} deg(u, \Gamma_0) = 1 - \sum_{c \in \Gamma_0} id_u(c), \\ \\ deg(u, \Gamma_i) = 1 + \sum_{c \in \Gamma_i} id_u(c), \quad \forall\, i \in [\![1, n_\Gamma]\!]. \end{cases} \tag{17}$$

where Γ_0 denotes the exterior boundary Ω. According to our experiments, while it can be easy to construct cross-fields that satisfy formula (16) (for example, by using formula (2)), generating cross-fields that conform to formula (17) in a simple and efficient manner proved to be more challenging. As an example, the cross-field shown in Figure 10 complies with condition (16), but does not with (17).

Therefore, we introduce an angle field ψ defined on Ω which will be used to correct the annular defect of the field u on the borders of each connected component. As outlined in Section 2.4, the ultimate cross field v is represented by:

$$v = R(\phi)R(\psi)u, \tag{18}$$

where $R(\phi)$ and $R(\psi)$ are rotation matrices corresponding to the angles ϕ (was defined in section 2.4) and ψ. The computation of ϕ in equation (14) has to be adjusted as follows:

$$\tilde{\phi} = \theta_N - \theta_u - \psi. \tag{19}$$

The angle field ψ acts as a correction factor for the angular defects caused by the presence of holes within the domain. To define it, we evaluate a subsidence vector

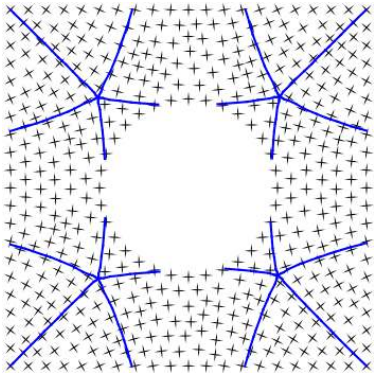

Fig. 10 Non-aligned cross-field

field h, whose angle θ_h is 4 times ψ. The vector field h is given by the following equation:

$$\begin{cases} \triangle h = 0, \\ \dfrac{1}{2\pi}\displaystyle\int_{\Gamma_0} \theta_h = 4\left(deg(u,\Gamma_0) - 1 + \sum_{c\in\Gamma_0} id_u(c)\right), \\ \dfrac{1}{2\pi}\displaystyle\int_{\Gamma_i} \theta_h = 4\left(deg(u,\Gamma_i) - 1 - \sum_{c\in\Gamma_i} id_u(c)\right), \\ \qquad\qquad \forall\, i \in [\![1, n_\Gamma]\!]. \end{cases} \tag{20}$$

In practice, we might need to modify h to remove possible singular points in h. We do this by using the formula (2).

The application of the method to the cross-field depicted in Figure 10 results in an aligned cross-field, as demonstrated in Figure 11. The resulting quadrilateral mesh can be seen in Figure 12.

Further visual representations of the results can be found in Figure 13.

As previously discussed in the introduction of section 3, we demonstrate an example of a multi-material geometry in Figure 14. The geometry is composed of a combination of two half-discs and a square plate with a circular hole. By utilizing the techniques developed earlier, specifically by addressing singular points on the boundary and treating domains with holes, we can produce a valid mesh.

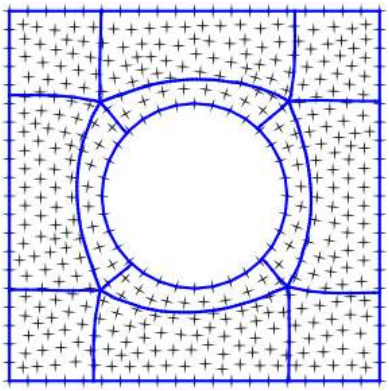

Fig. 11 Aligned cross-field

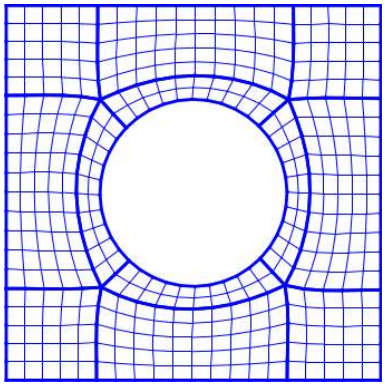

Fig. 12 Mesh quad on non-simply connected domain

4 Case of non-planar surfaces

In this section, let's apply the method presented in previous sections to non-planar surfaces. In particular, the lack of a global reference frame to compute the angles of the cross-field on non-planar surfaces is addressed. To overcome this challenge, we propose to utilize the heat method for diffusion as presented in [22]. This method propagates a given vector at a point accordingly to the heat equation. This allows for the construction of a global reference frame for the surface, which enables accurate computation of the angles of the cross-field and alignment with the boundary of the non-planar surface. More specifically, we construct a vector field w on the surface using equation (21), with homogeneous Neumann boundary conditions. We begin the resolution by initializing the equation with a vector field that is equal to an arbitrary vector in the tangent space of an arbitrary point and is set to zero everywhere else on the surface. By solving this equation over a very short time period, we obtain a vector field that does not have any singularities. The next step is to generate a frame

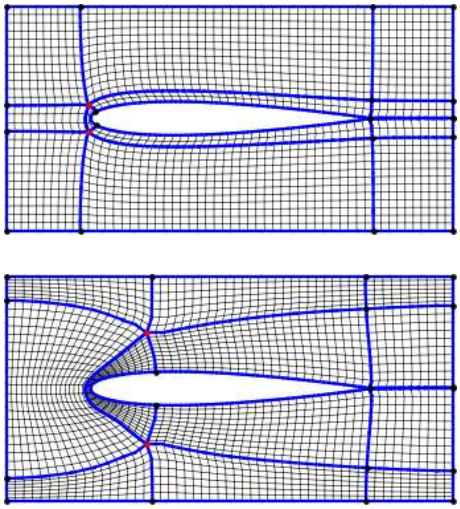

Fig. 13 Mesh of Naca0012 with two different configurations of singular points. The initial cross-fields were obtained using formula (2) by shifting the position of the internal singular points $(a_i)_{i\in 1,2}$ involved in the formula with $di = -1,\ \forall i$.

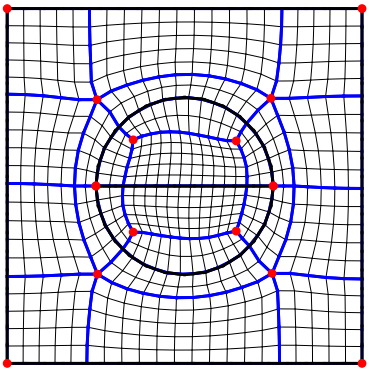

Fig. 14 An example with two connected components

at each point of the surface using formula 3.

$$\frac{\partial w}{\partial t} = \nabla^2 w, \tag{21}$$

Figure 15 shows an example of the solution of the equation and figure 16 illustrates the resulting global frame obtained.

In order to illustrate our method in the context of curved surfaces, we will present an adaptation of the process explained in section 2.4 on a quarter of a sphere.

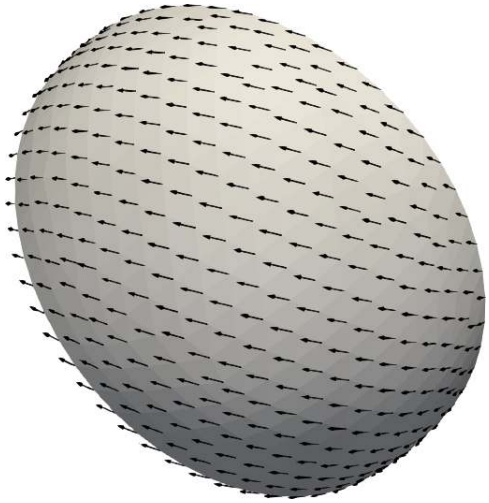

Fig. 15 Vector field obtained by the heat method diffusion [22].

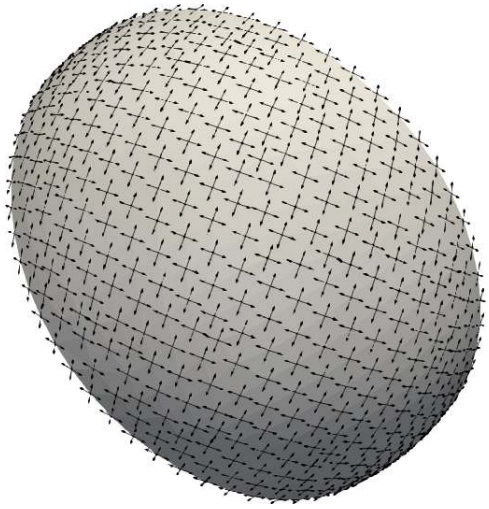

Fig. 16 Global frame.

We begin by defining a cross-field on the surface, using the same approach as described in section 2.4 and depicted on Figure 5. The outcome is displayed in Figure 17. However, similar to the scenario presented in section 2.4, this cross-field may not be in sync with the boundary of the domain, leading to domains that are not four-sided.

To overcome this problem, we adjust the cross-field as described in section 2.4. The outcome of this adjustment on the example of a quarter of a sphere is illustrated in Figure 18.

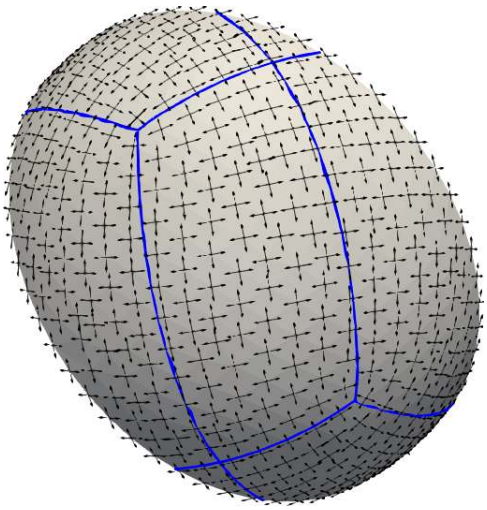

Fig. 17 Invalid partitioning.

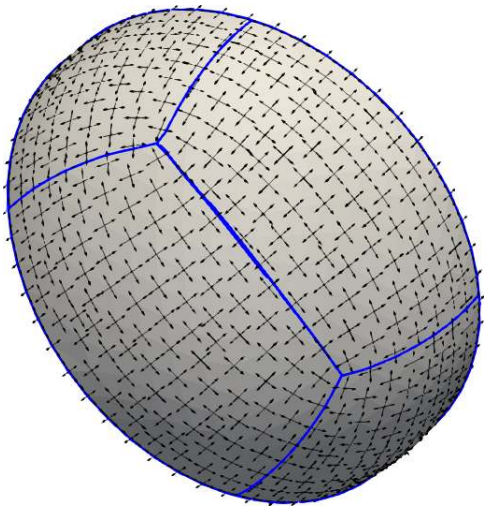

Fig. 18 Rectified cross-field.

Finally, the quadrilateral mesh is obtained by meshing each block with four sides, and it is shown in Figure 19.

Other examples of the results obtained on various geometries are presented in Figure 20.

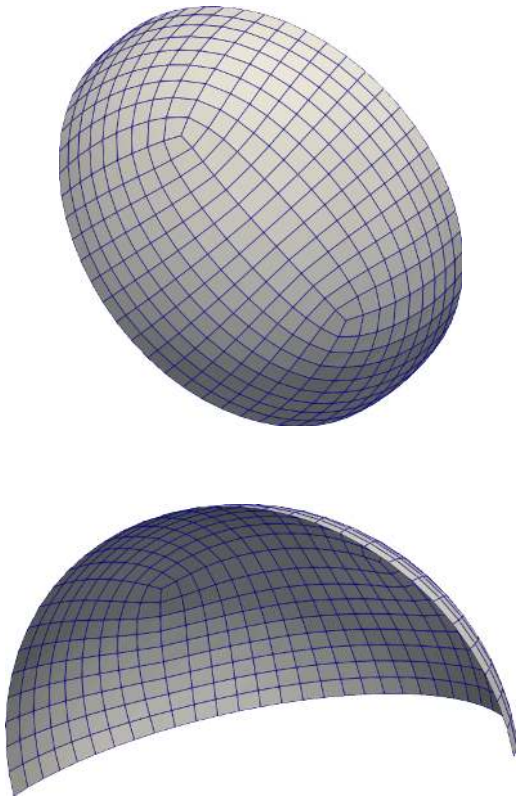

Fig. 19 Quadrilateral mesh of the quarter-sphere

5 Conclusion

We have presented a method that allows to abstract the construction of the mesh from the generation of the cross-field. The field of crosses is given by respecting constraints that we have shown. It is then modified in order to adapt it to the topology of the domain. The advantage is that we benefit from a different distribution of singular points, and that we can easily take into account non-planar surface manifolds. We have also implemented operations to take into account arbitrary indexes of singular points of boundary and also non simply connected domains. In a future work, we hope to extend the method to mesh adaptation with respect to the solution of a given equation.

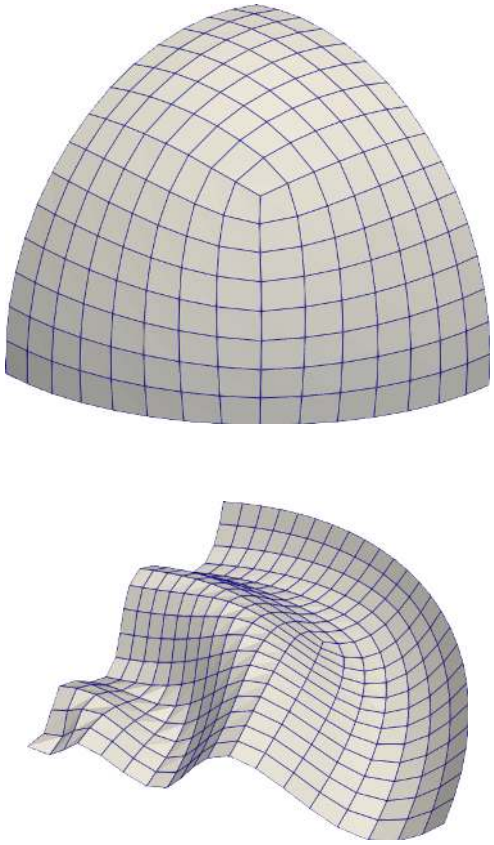

Fig. 20 Other examples of quadrilateral meshes on non planar geometries

Acknowledgments

The authors are grateful to anonymous referees for their helpful comments and suggestions.

References

1. M. Reberol, Maillages hex-dominants : génération, simulation et évaluation. Ph.D. thesis (2018)
2. N. Kowalski, F. Ledoux, P. Frey, in *21th Int. Meshing Roundtable* (Sandia Natl. Labs., San Jose, United States, 2012). URL https://hal.sorbonne-universite.fr/hal-01076754
3. D. Bommes, B. Levy, N. Pietroni, E. Puppo, C. Silva, D. Zorin, Computer Graphics Forum **32** (2013). DOI 10.1111/cgf.12014
4. T. Gurung, D. Laney, P. Lindstrom, J. Rossignac, Comput. Graph. Forum **30**, 355 (2011). DOI 10.1111/j.1467-8659.2011.01866.x

5. J.F. Remacle, J. Lambrechts, B. Seny, E. Marchandise, A. Johnen, C. Geuzaine, International Journal for Numerical Methods in Engineering **89**, 1102 (2012). DOI 10.1002/nme.3279
6. R. Schneiders, Engineering with Computers **12**, 168 (2005)
7. T.D. Blacker, M.B. Stephenson, International Journal for Numerical Methods in Engineering **32**(4), 811 (1991). DOI https://doi.org/10.1002/nme.1620320410
8. M. Staten, R. Kerr, S. Owen, T. Blacker, M. Stupazzini, K. Shimada, International Journal for Numerical Methods in Engineering - INT J NUMER METHOD ENG **81** (2009). DOI 10.1002/nme.2679
9. D.L. Rigby, (2003)
10. T.K.H. Tam, C.G. Armstrong, Advances in Engineering Software and Workstations **13**, 313 (1991)
11. N. Ray, B. Vallet, W.C. Li, B. Lévy, ACM Trans. Graph. **27**(2) (2008). DOI 10.1145/1356682.1356683. URL https://doi.org/10.1145/1356682.1356683
12. D. Bommes, H. Zimmer, L. Kobbelt, ACM Trans. Graph. **28**(3) (2009). DOI 10.1145/1531326.1531383. URL https://doi.org/10.1145/1531326.1531383
13. M. Nieser, U. Reitebuch, K. Polthier, Computer Graphics Forum **30**(5), 1397 (2011). DOI https://doi.org/10.1111/j.1467-8659.2011.02014.x
14. K.M. Shepherd, X.D. Gu, T.J. Hughes, Computer Methods in Applied Mechanics and Engineering **402**, 115555 (2022)
15. N. Lei, X. Zheng, Z. Luo, F. Luo, X. Gu, Computer methods in applied mechanics and engineering **366**, 112980 (2020)
16. R. Viertel, B. Osting. An approach to quad meshing based on harmonic cross-valued maps and the ginzburg-landau theory (2018)
17. P.A. Beaufort, J. Lambrechts, F. Henrotte, C. Geuzaine, J.F. Remacle, Procedia Engineering **203**, 219 (2017). DOI https://doi.org/10.1016/j.proeng.2017.09.799. 26th International Meshing Roundtable, IMR26, 18-21 September 2017, Barcelona, Spain
18. J. Jezdimirović, A. Chemin, M. Reberol, F. Henrotte, J. François Remacle, arXiv e-prints arXiv:2103.02939 (2021)
19. A. Macq, M. Reberol, F. Henrotte, P.A. Beaufort, A. Chemin, J.F. Remacle, J.V. Schaftingen. Ginzburg-landau energy and placement of singularities in generated cross fields (2020)
20. W.A. Cook, International Journal for Numerical Methods in Engineering **8**(1), 27 (1974)
21. N. Ray, B. Vallet, W.C. Li, B. Lévy, ACM Trans. Graph. **27**(2) (2008). DOI 10.1145/1356682.1356683. URL https://doi.org/10.1145/1356682.1356683
22. N. Sharp, Y. Soliman, K. Crane, ACM Transactions on Graphics (TOG) **38**(3), 1 (2019)